Structural Engineering and Mechanics, *Vol. 73, No. 2 (2020) 133-141*
DOI: https://doi.org/10.12989/sem.2020.73.2.133

Series tuned mass dampers in vibration control of continuous railway bridges

Onur Araz*[1] and Volkan Kahya[2a]

[1]*Department of Civil Engineering, Gümüşhane University, Gümüşhane 29100, Turkey*
[2]*Department of Civil Engineering, Karadeniz Technical University, Trabzon 61080, Turkey*

(Received June 12, 2019, Revised September 26, 2019, Accepted September 27, 2019)

Abstract. This paper presents the applicability of series tuned mass dampers (STMDs) to reduce the multiple resonant responses of continuous railway bridges under high-speed train. The bridge is modeled by two-span Bernoulli-Euler beam with uniform cross-section, and a STMD device consisting of two TMD units installed on the bridge to reduce its multiple resonant vibrations. The system is assumed to be under the action of a high-speed train passage which is modeled as a series of moving forces. Sequential Programming Technique (SQP) is carried out to find the optimal parameters of the STMD that minimizes the maximum peak responses of the bridge. Comparisons with the results available in the literature are presented to demonstrate the effectiveness and robustness of STMD system in reducing the multiple resonant responses of the continuous railway bridges under high-speed trains.

Keywords: high-speed train; multiple resonance; railway bridge; series tuned mass damper; vibration control

1. Introduction

Resonant vibrations of a bridge excited by a train is an interesting topic for structural engineers. When successive moving loads with high velocity travel on bridges, they may suffer from excessive vibrations that can seriously affect the comfort of passengers and bridge's structural performance (Adam and Salcher 2014, Podworna 2017). Various control systems can be developed for suppressing the resonant vibrations. Among them, the use of passive tuned mass dampers is very simple and economic. This property has rendered the tuned mass dampers (TMDs) attractive to researchers. Therefore, there is a vast literature about reducing the resonant responses of bridges due to moving trains by TMDs. Therein, the general purpose is to obtain the optimum parameters of TMD device to provide it to work with its best performance. For example, Wang *et al*. (2003), Li *et al*. (2005), Wu (2006), Moghaddas *et al*. (2012), Samani *et al*. (2013), Rostam *et al*. (2015) and Miguel *et al*. (2016) obtained the optimum parameters of the vibration absorber for suppressing the resonant response of single-span simply supported beams. In these studies, the absorber is considered as either a single or a multiple tuned mass damper (MTMD) in which the TMD units are connected each other in parallel, and it was installed at the midspan of the beam. Unlike the above-mentioned works, Yau and Yang (2004a,b) and Luu *et al*. (2012) studied the multiple resonant peaks of train-induced vibrations of continuous railway bridges by using a MTMD system.

Series tuned mass dampers (STMDs) are another form of multiple tuned mass dampers in which the TMD units are connected each other in series. Most of the previous work on the STMDs is concerned with the reduction of structural vibrations under the ground acceleration and base excitations (Li and Zhu 2006, Zuo 2009, Asami 2017, Asami *et al*. 2018). Only Kahya and Araz (2017) investigated the application of STMDs in suppressing the resonant vibrations of simply supported single-span bridges under moving loads.

Recently, the tuned mass damper inerter (TMDI) is developed and used to control the vibrations of engineering structures (Giaralis and Petrini 2017, Ruiz *et al*. 2018, Xu *et al*. 2019).

As seen in the above-given literature review, the investigations on reduction of the first resonant responses of bridges were carried out by a number of researchers. This is not, however, sufficient for multi-span bridges, because they have multiple resonant peaks. To the best of the authors' knowledge, there is no study in which a STMD device have been used to control the multiple resonant peaks of a continuous railway bridge. Thus, this paper deals with the optimization and applicability of STMDs to reduce the multiple resonant peaks of a continuous bridge under high speed trains. For this purpose, two-span elastic beam under the action a series of moving loads is considered as the continuous beam-train model. A STMD consisting of two TMD units, one has greater mass than the other, is installed on the beam. Optimum properties of the STMD are obtained by using the Sequential Programming Technique (SQP) based on the minimization of the maximum resonant responses of the bridge.

*Corresponding author, Assistant Professor, Ph.D.
E-mail: onuraraz29@hotmail.com
[a] Professor
E-mail: volkan@ktu.edu.tr

ISSN: 1225-4568 (Print), 1598-6217 (Online)

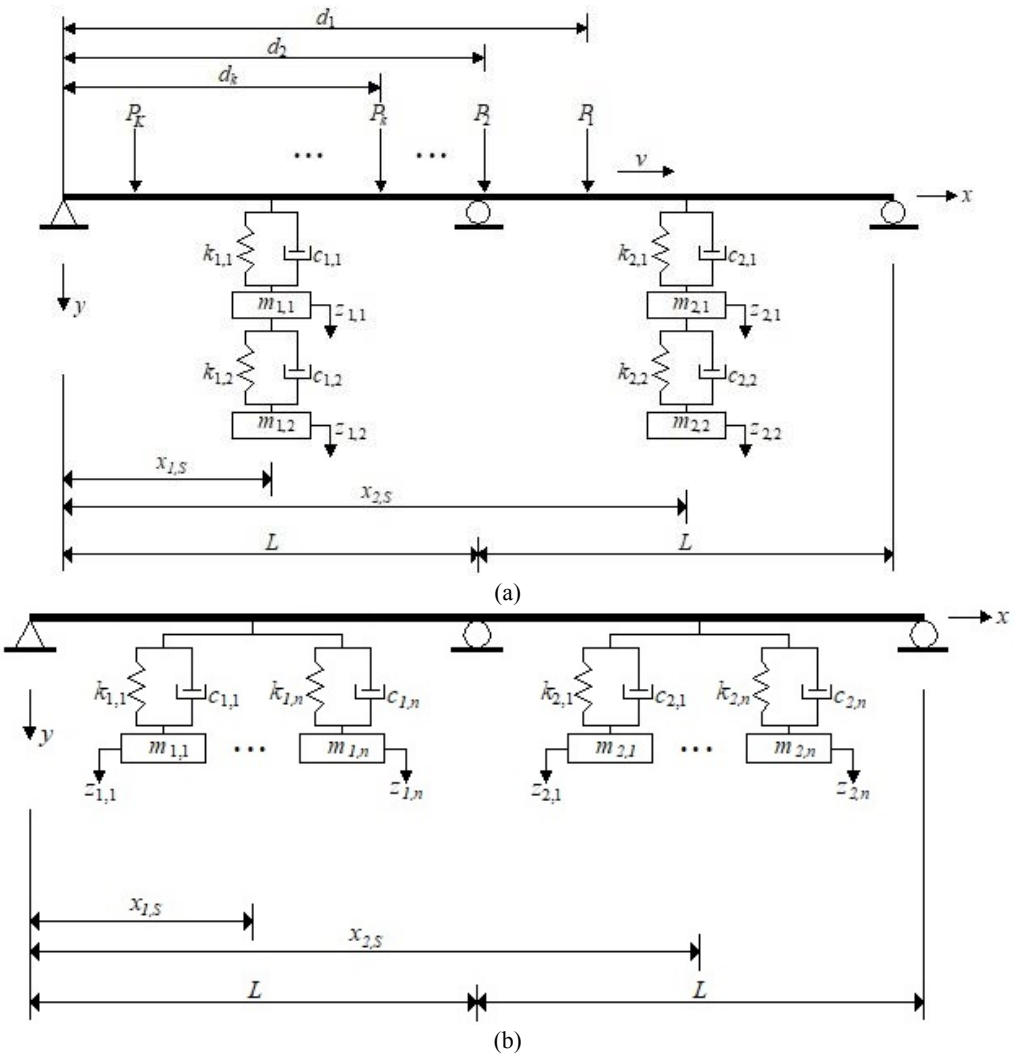

Fig. 1 Two-span bridge installed with TMDs under train loads: (a) STMD-4 and (b) MTMD-2*n*

2. Mathematical formulation

The system configuration consists of a two-span continuous bridge with a STMDs and the number *n* of the TMDs units contained in MTMD system installed at the middle of each span as shown in Fig. 1.

Each STMD device consists of two TMD units connected each other in series, thus we refer to this system as STMD-4 which means there are four TMD units installed on the bridge.

Equation of motion for the bridge with STMD-4 and high-speed train shown in Fig. 1 can be written as (Wang *et al*. 2010)

$$EIy^{IV}(x,t)+m_b\ddot{y}(x,t)+c_b\dot{y}(x,t)=F_v(x,t)+F_T(x,t) \quad (1)$$

where $y(x,t)$, EI, m_b and c_b denote the displacement, the flexural stiffness, the mass per unit length and the damping of the beam, respectively. Primes and dot denote the derivative with respect to x and t, respectively. $F_v(x,t)$ and $F_T(x,t)$ are the external forces acting on the bridge due to the train and the STMD systems, respectively. $F_v(x,t)$ can be defined as

$$F_v(x,t)=\sum_{k=1}^{K}P_k\delta(x-x_k)\left[H\left(t-t_k\right)-H\left(t-t_k-\Delta t\right)\right] \quad (2)$$

where x_k is the distance of the kth load from the left-hand end of the continuous beam, $t_k = x_k / v$ is the arrival time of the kth load at the beam, $\Delta t = 2L / v$ is the time of the load passing the beam, K is total number of axle forces, P_k is the magnitude of the kth axle force, δ(-) is Dirac delta function and H(-) is Heaviside unit step function. $F_T(x,t)$ can be defined as follows

$$F_T(x,t)=F_{T,1}(x,t)+F_{T,2}(x,t) \quad (3)$$

where $F_{T,1}(x,t)$ and $F_{T,2}(x,t)$ are the forces acting on the bridge from the STMDs at the first and second midspans, respectively, as

$$F_{T,1}(x,t)=\begin{Bmatrix}c_{1,1}\left[\dot{z}_{1,1}(t)-\dot{y}(x_{s,1},t)\right]+\\ k_{1,1}\left[z_{1,1}(t)-y(x_{s,1},t)\right]\end{Bmatrix}\delta(x-x_{s,1}) \quad (4)$$

$$F_{T,2}(x,t)=\begin{Bmatrix}c_{2,1}\left[\dot{z}_{2,1}(t)-\dot{y}(x_{s,2},t)\right]+\\ k_{2,1}\left[z_{2,1}(t)-y(x_{s,2},t)\right]\end{Bmatrix}\delta(x-x_{s,2}) \quad (5)$$

where $x_{s,1}$ and $x_{s,2}$ denote the installation points of the

STMDs, respectively.

Equations of motion for the STMD at the first span can be written as

$$\begin{aligned} &m_{1,1}\ddot{z}_{1,1}(t)+c_{1,1}\left[\dot{z}_{1,1}(t)-\dot{y}(x_{s,1},t)\right]+\\ &k_{1,1}\left[z_{1,1}(t)-y(x_{s,1},t)\right]-m_{1,2}\ddot{z}_{1,2}=0 \end{aligned} \tag{6}$$

$$m_{1,2}\ddot{z}_{1,2}(t)+c_{1,2}\left[\dot{z}_{1,2}(t)-\dot{z}_{1,1}(t)\right]+k_{1,2}\left[z_{1,2}(t)-z_{1,1}(t)\right]=0 \tag{7}$$

where $z_{1,1}$, $m_{1,1}$, $c_{1,1}$ and $k_{1,1}$ are the displacement, mass, damping and stiffness of the first TMD unit, $z_{1,2}$, $m_{1,2}$, $c_{1,2}$ and $k_{1,2}$ are the displacement, mass, damping and stiffness of the second TMD unit in the first STMD, respectively.

Equations of motion for the STMD at the second midspan can be written as

$$\begin{aligned} &m_{2,1}\ddot{z}_{2,1}(t)+c_{2,1}\left[\dot{z}_{2,1}(t)-\dot{y}(x_{s,2},t)\right]+\\ &k_{2,1}\left[z_{2,1}(t)-y(x_{s,2},t)\right]-m_{2,2}\ddot{z}_{2,2}=0 \end{aligned} \tag{8}$$

$$\begin{aligned} &m_{2,2}\ddot{z}_{2,2}(t)+c_{2,2}\left[\dot{z}_{2,2}(t)-\dot{z}_{2,1}(t)\right]+\\ &k_{2,2}\left[z_{2,2}(t)-z_{2,1}(t)\right]=0 \end{aligned} \tag{9}$$

where $z_{2,1}$, $m_{2,1}$, $c_{2,1}$ and $k_{2,1}$ are the displacement, mass, damping and stiffness of the first TMD unit, $z_{2,2}$, $m_{2,2}$, $c_{2,2}$ and $k_{2,2}$ are the displacement, mass, damping and stiffness of the second TMD unit in the second STMD, respectively.

Assume the displacement of the bridge as

$$y(x,t)=\sum_{i=1}^{N}q_i(t)\varphi_i(x) \tag{10}$$

where N is the number of modes, $q_i(t)$ is the generalized coordinate of ith vibration mode of the bridge and $\varphi_i(x)$ is modal shape function for the ith mode. Substituting Eq. (10) into Eq. (1), multiplying the resulting expression by $\varphi_m(x)$, carrying out the integration with respect to 0 and $2L$, and using the modal orthogonality, the ith modal equation of motion for the system can be obtained as

$$\ddot{q}_i+2\tilde{\xi}_i\tilde{\omega}_i\dot{q}_i+\tilde{\omega}_i^2q_i=F_{vi}+F_{Ti} \tag{11}$$

where $\tilde{\xi}_i$ and $\tilde{\omega}_i$ are the damping ratio and natural frequency for the ith mode of beam vibrations, respectively.

The ith modal force F_{vi} induced by the train is expressed as

$$F_{vi}(x,t)=\frac{1}{M_i}\sum_{k=1}^{K}P_k\varphi_i(x_k)\left[H\left(t-t_k\right)-H\left(t-t_k-\Delta t\right)\right] \tag{12}$$

and the ith modal force F_{Ti} induced by STMDs are

$$\begin{aligned} F_{Ti}(x,t)=&\left\{\begin{array}{l} c_{1,1}\left[\dot{z}_{1,1}(t)-\sum_{m=1}^{N}\dot{q}_m\varphi_m(x_{s,1})\right]+\\ k_{1,1}\left[z_{1,1}(t)-\sum_{m=1}^{N}q_m\varphi_m(x_{s,1})\right] \end{array}\right\}\frac{\varphi_i(x_{s,1})}{M_i}+\\ &\left\{\begin{array}{l} c_{2,1}\left[\dot{z}_{2,1}(t)-\sum_{m=1}^{N}\dot{q}_m\varphi_m(x_{s,2})\right]+\\ k_{2,1}\left[z_{2,1}(t)-\sum_{m=1}^{N}q_m\varphi_m(x_{s,2})\right] \end{array}\right\}\frac{\varphi_i(x_{s,2})}{M_i} \end{aligned} \tag{13}$$

where M_i is the modal mass of ith mode and it can be written as

$$M_i=\int_0^{2L}m_b\varphi_i^2(x)dx \tag{14}$$

where m_b is the constant mass per unit length of the bridge, and φ_i is the nth modal shape function of the bridge.

Substituting Eq. (10) into Eqs. (6) and (8), we have the followings:

$$\begin{aligned} &m_{1,1}\ddot{z}_{1,1}(t)+c_{1,1}\left[\dot{z}_{1,1}(t)-\sum_{m=1}^{N}\dot{q}_m\varphi_m(x_{s,1})\right]+\\ &k_{1,1}\left[z_{1,1}(t)-\sum_{m=1}^{N}q_m\varphi_m(x_{s,1})\right]-m_{1,2}\ddot{z}_{1,2}=0 \end{aligned} \tag{15}$$

$$\begin{aligned} &m_{2,1}\ddot{z}_{2,1}(t)+c_{2,1}\left[\dot{z}_{2,1}(t)-\sum_{m=1}^{N}\dot{q}_m\varphi_m(x_{s,2})\right]+\\ &k_{2,1}\left[z_{2,1}(t)-\sum_{m=1}^{N}q_m\varphi_m(x_{s,2})\right]-m_{2,2}\ddot{z}_{2,2}=0 \end{aligned} \tag{16}$$

Eqs. (7), (9), (11), (15) and (16) constitute a system of coupled second-order differential equations that can be solved by direct numerical integration. Here, the Newmark method is used to solve the above equations taking the first five modes of the bridge into account (β = 1/4 and γ = 1/2).

3. Sequential programming technique

The optimization problem considered is solved by means of a gradient-based constrained optimization algorithm implemented in the MATLAB Optimization Toolbox (Matlab, R2015b) which uses Sequential Programming Technique (SQP). The flowchart of SQP technique is presented in Fig. 2. The SQP technique consists of three main stages:

1) Calculate an approximation of the Hessian matrix of the Lagrangian function using quasi-Newton method.

2) Calculate a formulation of the quadratic programming (QP) problem.

3) Calculate a line search and objective function.

Maximum displacement at the second midspan is considered as an objective function, and the fmincon is applied to find out simultaneously the optimal parameters of STMDs.

For the sake of numerical stability, the following dimensionless variables for STMDs are defined:

$$\begin{aligned} &\xi_{1,1}=\frac{c_{1,1}}{2m_{1,1}\omega_{1,1}},\ \xi_{1,2}=\frac{c_{1,2}}{2m_{1,2}\omega_{1,2}},\ \xi_{2,1}=\frac{c_{2,1}}{2m_{2,1}\omega_{2,1}},\\ &\xi_{2,2}=\frac{c_{2,2}}{2m_{2,2}\omega_{2,2}},\ \mu_1=\frac{m_{1,1}}{mL},\ \mu_2=\frac{m_{1,2}}{mL},\ \mu_3=\frac{m_{2,1}}{mL},\\ &\mu_4=\frac{m_{2,2}}{mL},\ \mu_{1T}=\frac{\mu_2}{\mu_1},\ \mu_{2T}=\frac{\mu_4}{\mu_3},\ \mu_T=\frac{\mu_1+\mu_2}{\mu_3+\mu_4},\\ &f_{1,1}=\frac{\omega_{1,1}}{\bar{\omega}_1},\ f_{1,2}=\frac{\omega_{1,2}}{\bar{\omega}_1},\ f_{2,1}=\frac{\omega_{2,1}}{\bar{\omega}_1},\ f_{2,2}=\frac{\omega_{2,2}}{\bar{\omega}_1} \end{aligned} \tag{17}$$

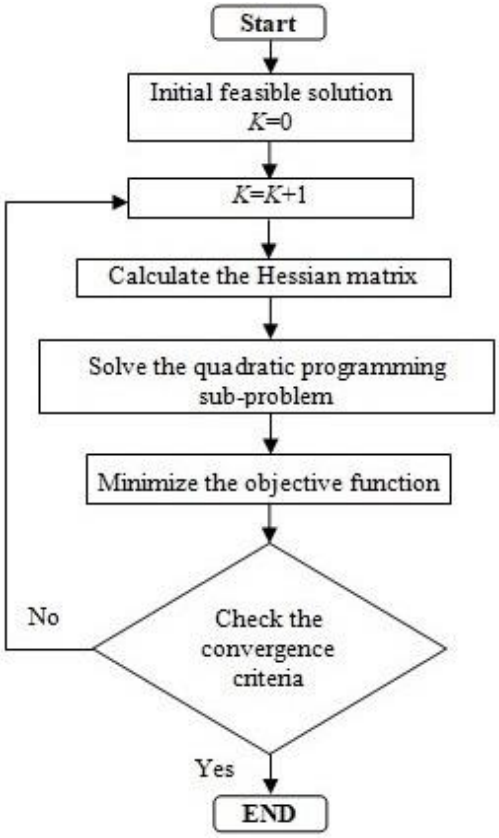

Fig. 2 The flowchart of SQP technique

where $f_{1,1}$, $f_{1,2}$, $f_{2,1}$ and $f_{2,2}$ are the frequency ratios, $\xi_{1,1}$, $\xi_{1,2}$, $\xi_{2,1}$ and $\xi_{2,2}$ are the damping ratios, $\omega_{1,1}$, $\omega_{1,2}$, $\omega_{2,1}$ and $\omega_{2,2}$ are the natural frequencies, and μ_1, μ_2, μ_3 and μ_4 are the mass ratios of each TMD in STMD devices, respectively.

μ_{1T} and μ_{2T} are the mass ratios of the smaller TMD to the larger one in STMDs, respectively. $\mu = \sum_{j=1}^{4} \mu_j$ is the total mass ratio.

Within the present concerns, the optimization problem might be basically stated as follows:

$$\min J(q) \quad \text{with} \quad l_b \le q \le u_b \tag{18}$$

where q, $J(q)$, l_b and u_b represent the optimization variables, objective function, lower and upper bounds of the optimization variables, respectively. The following ranges are selected for the control parameters of STMDs. The search increment for the variable parameter and objective function set to be 10^{-6}.

$$\begin{aligned} q &= [\xi_{1,1}, \xi_{1,2}, \xi_{2,1}, \xi_{2,2}, f_{1,1}, f_{1,2}, f_{2,1}, f_{2,2}, \mu_{1T}, \mu_{2T}, \mu_T], \\ l_b &= [0, 0, 0, 0, 0.8, 0.8, 0.8, 0.8, 0, 0, 0], \\ u_b &= [0.5, 0.5, 0.5, 0.5, 1.8, 1.8, 1.8, 1.8, 1, 1, 1] \end{aligned} \tag{19}$$

4. Numerical results

To suppress the multiple resonant peaks of a two-span continuous bridge with different TMD systems, some illustrated examples are presented in this section. For numerical analyses, each span of the beam with constant cross section is modeled as a Bernoulli-Euler beam with the following properties: L = 20m, EI = 2.5×10^{10} Nm^2, m_b = 34,088 kg/m, ξ = 0.025 (Wang *et al*. 2010). To study the phenomenon of train-induced resonance on railway bridges, a train is often simulated as a series of moving loads with regular intervals (Yau *et al*. 2001, Luu *et al*. 2014). Wang *et al*. (2003) also indicate that the use of the different train models brings about a change in resonant train speeds about 2.5%. Thus, the effects of vehicle–structure interaction are neglected in this paper. The high-speed train model HSLM-A8 is used in numerical analyses, which is one of the high-speed passenger train models in Eurocode 1 (refer to Table 1). The resonant speeds of a train are dependent upon two factors: the modal frequencies of the bridge and the load spacing of the train (Wang *et al*. 2003). Resonant or critical speeds of a train are thus given by

$$v_{i,p} = \frac{\tilde{\omega}_i d}{2\pi p}, \quad p = 1, 2, 3, \ldots \tag{20}$$

where $\tilde{\omega}_i$ and d are ith the natural circular frequency of the bridge and the distance between two bogies or a length of the coach, respectively, p denotes the resonant number.

The maximum displacements computed for the each midspan of the continuous beam is plotted against the different train speeds from 100 km/h to 600 km/h in Fig. 3. As seen, there are two resonant peaks on the bridge when the train speeds are close to 300 km/h and 470 km/h, respectively. With the first two natural circular frequencies of the bridge $\tilde{\omega}_1 = 21.13$ rad/s and $\tilde{\omega}_2 = 33.03$ rad/s, the

Table 1 Properties of the HSLM-A high-speed trains

Universal train	Number of intermediate coaches, N	Coach length (m)	Bogie axle spacing (m)	Point force (kN)
HSLM-A7	13	24	2	190
HSLM-A8	12	25	2.5	190
HSLM-A9	11	26	2	210

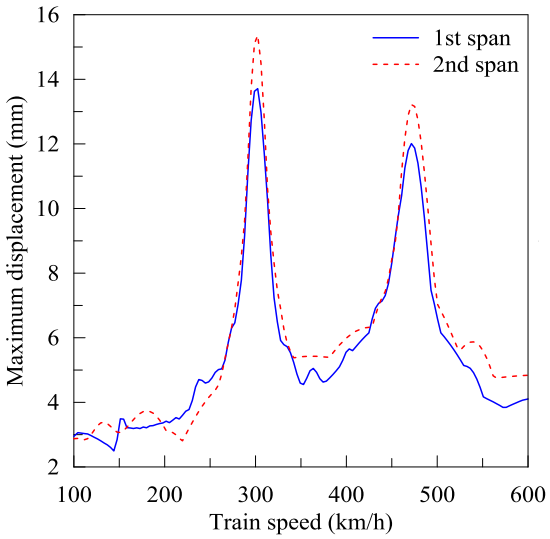

Fig. 3 Maximum displacements under the train passage

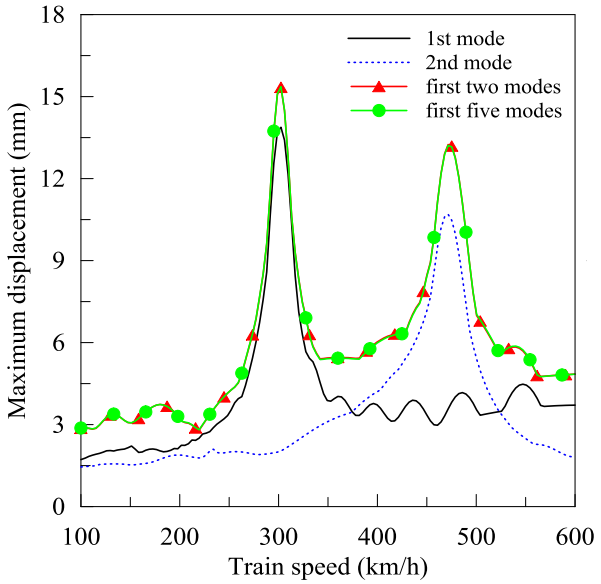

Fig. 4 Effect of different modes on the maximum displacement of bridge at the second midspan

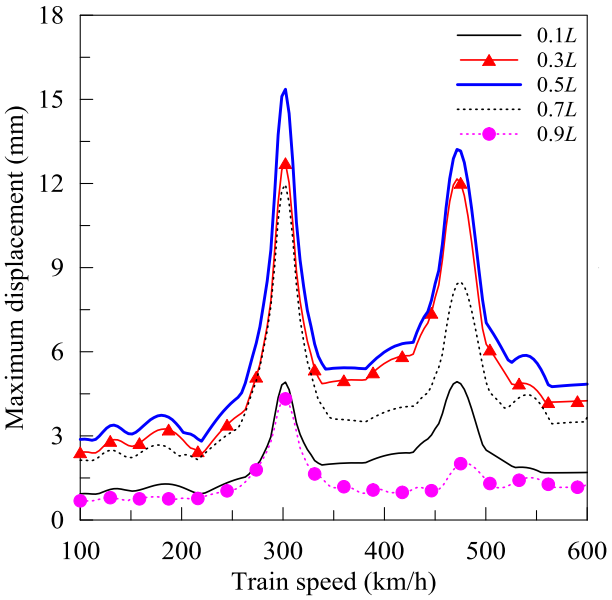

Fig. 5 Effect of different locations on the maximum displacement of bridge at the second midspan

corresponding resonant speeds of the train according to Eq.(20) are 302.7 km/h and 472.9 km/h, respectively.

Fig. 3 also indicates that the maximum displacement of the second span is larger than the first one for both critical speeds. Therefore, only the response of the second midspan is considered. In addition, the two-span continuous beam has two resonant peaks. Thus, two different STMDs are used in order to reduce the two resonant peaks.

Contribution of different modes on the maximum displacements at the second midspan of the bridge is shown in Fig. 4. As seen, first two modes that dominate the total response of the bridge are very important to compute the displacement response of the considered two-span continuous bridge under moving train. Thus, in the study, the STMDs are designed to control the first two modes of vibration of the bridge.

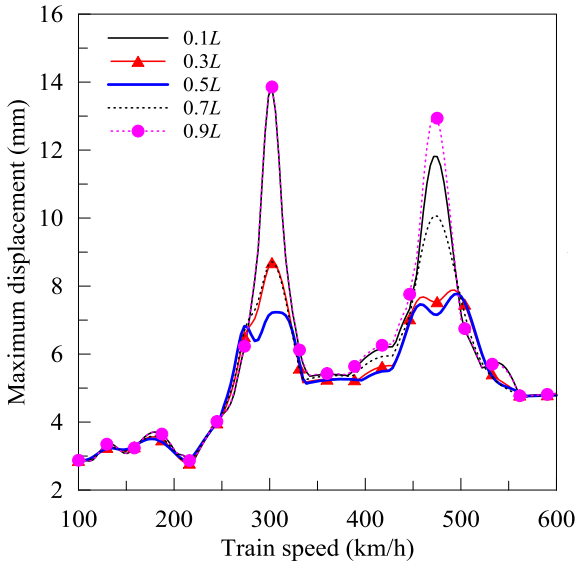

Fig. 6 Effect of location of the installation on the effectiveness of the STMD

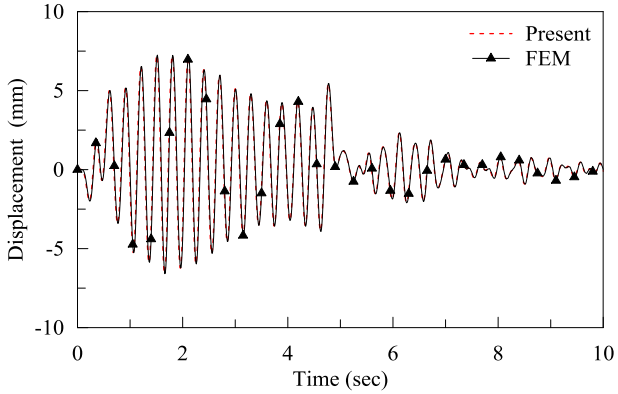

Fig. 7 Comparison of the analytical and numerical dynamic analysis results for dynamic vertical displacements of the second midspan with speed of 302.7 km/h

Table 2 Optimal parameters for various types of TMD systems with 2% total mass ratio

Type	No	x_s/L_t	fi	ξ_i (%)	μ_i (%)
STMD-4	1	1/4	1.372	0.000	0.575
	2	1/4	1.193	10.810	0.135
	3	3/4	1.373	0.000	1.126
	4	3/4	1.539	13.310	0.164
MTMD-4	1	1/4	0.949	2.872	0.775
(Luu *et al.* 2012)	2	1/4	1.035	3.132	0.651
	3	3/4	1.553	4.699	0.289
	4	3/4	1.556	4.737	0.285
TMD-2	1	1/4	0.987	4.553	1.421
(Luu *et al.* 2012)	2	3/4	1.546	7.128	0.579

Note: x_s is the distance of the ith TMD to the left-hand end of the continuous beam, L_t is total length of the continuous bridge, fi, ξ_i and μ_i are the optimal frequency, damping and mass ratio of the ith TMD

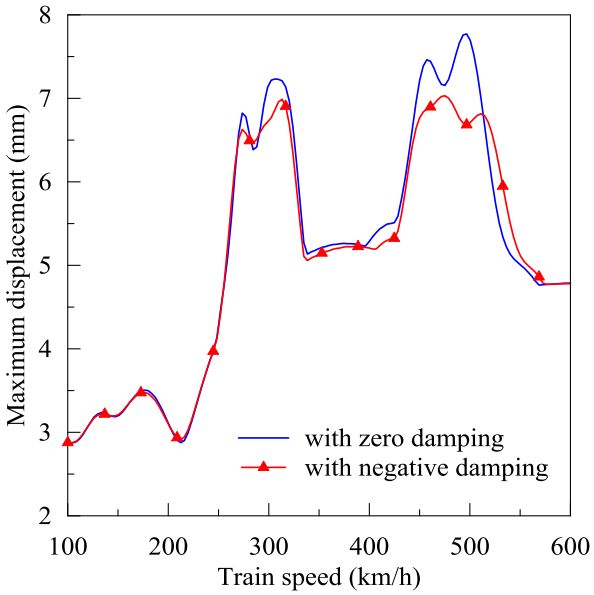

Fig. 8 Variation of displacement response for different optimization cases

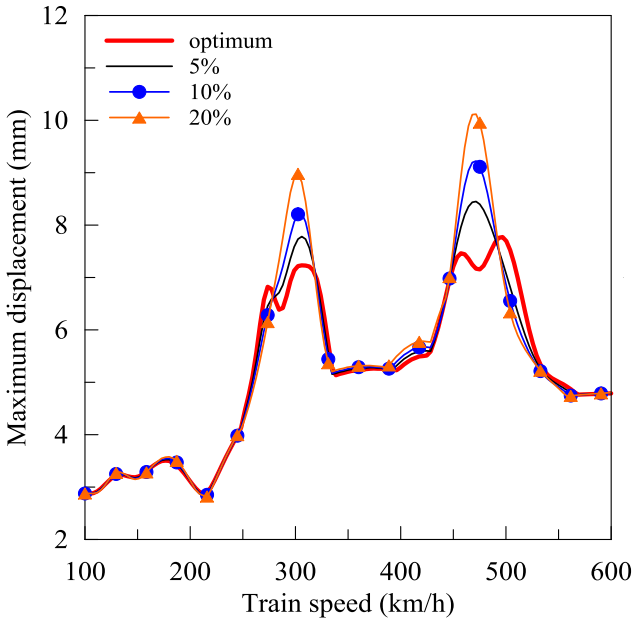

Fig. 9 Variation of displacement response for different damping ratio of the first TMD in STMD

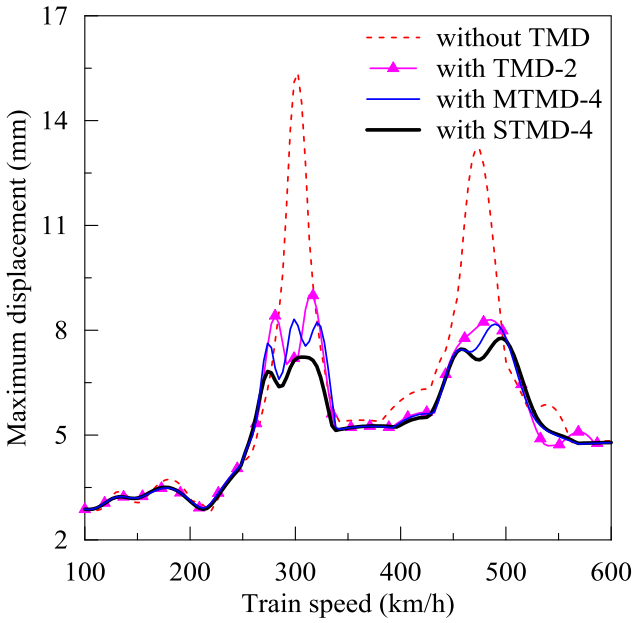

Fig. 10 Maximum displacements of second midspan of the bridge with optimum absorbers

Maximum displacements at different locations of the bridge is shown in Fig. 5. As seen, the displacement response at the midpoint of second span of the bridge is maximum. Fig. 5 also indicates that the displacement response decreases in the locations closer to the supports.

Effect of location of the STMD is investigated in Fig. 6. Here, maximum displacements of the second span are shown when the STMD is installed on different locations. As clearly seen, the optimal location is obtained as the middle of the span, i.e., 0.5L. This conclusion is consistent with that of previous works by Wang (2003), Luu *et al.* (2012), and Yau and Yang (2004a,b).

In Fig. 7, the midpoint deflection time-history of two-span bridge with single TMD on each span for undamped case is given. TMD parameters are selected as m = 6.82 t, c = 14.41 kNs/m and k = 3044 kN/m. Analytical results are compared with that of the finite element method (FEM) solutions obtained by SAP2000 software (CSI). TMD is modeled via a link element in SAP2000. As can be seen, the results obtained for both methods perfectly agree very well with each other.

When the lower and upper bounds for all of the optimization variables in Eq. (19) are limited to non-negative values, the optimum damping ratio of the first TMD in STMD device is equal to zero. If negative damping ratio is allowed in the optimization process, the optimum damping ratio of the first TMD becomes a negative value. The maximum displacements of the bridge with optimal STMD for the zero and negative damping cases are compared in Fig. 8. As can be seen, the best effectiveness of the STMD is obtained when the damping coefficient of the first TMD gets negative value, which means an active damper need to be added to the TMD unit. Even so, negative damping cannot be obtained for the passive vibration control (Asami, 2017). Thus, the damping constant of the first TMD must be configured to be zero.

The optimal parameters for STMD-4 and MTMD-4 from Luu *et al.* (2012) are given in Table 2. For STMD-4, optimum parameters are obtained by SQP while H_2 procedure was used for MTMD-4 which consists of four parallel connected TMD units. As seen, in STMDs, the optimum damping ratio of the first TMD is equal to zero. Thus, there is no need for the damping element in the first TMD in the STMD system. This finding is the same as those found by Li and Zhu (2006), Zuo (2009), Kahya and Araz (2017), Asami (2017) and Asami *et al.* (2018). It is also found that the optimum damping ratios obtained for the smaller TMD in STMDs are significantly larger than those of each TMD unit in MTMD-4 system. Optimum frequency ratios vary from 1.193 to 1.539 for STMD-4 while 0.949 to 1.556 for MTMD-4.

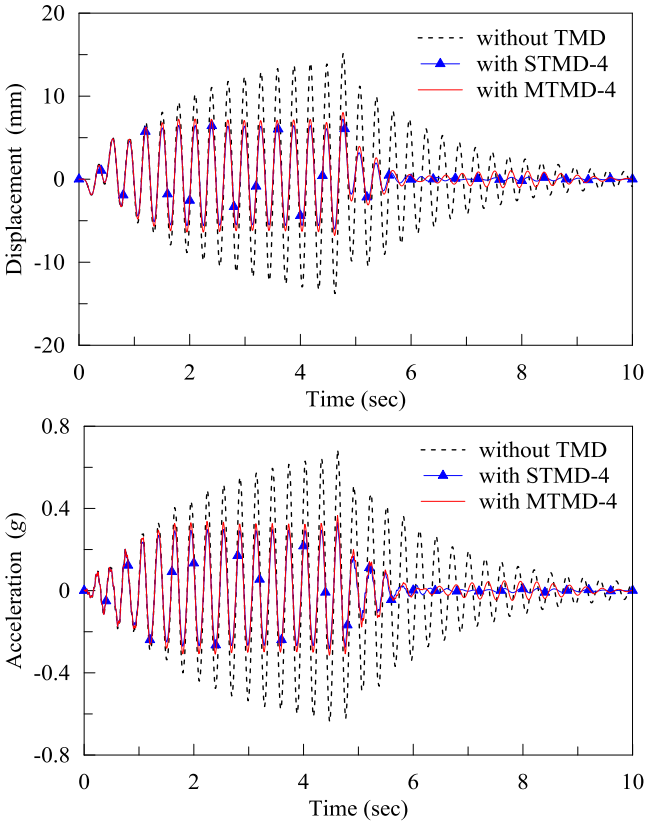

Fig. 11 Time histories of the second midspan of the bridge for the speed of 302.7 km/h

Fig. 9 presents the variation of displacement response against damping ratio of first TMD unit in STMD. As can be seen, the effectiveness of STMD decreases with the increase in the damping ratio of the first TMD. We also observe here that the smallest responses are obtained in case of zero-damping in the first TMD unit. Another observation from this figure, the optimal STMDs are very effective in reducing dynamic responses of bridge during resonant speeds. But their effectiveness rapidly decreases when the optimum design parameters of STMDs are changed.

Fig. 10 shows the variation of maximum displacements of the bridge with regard to the train speed for three optimum TMDs (i.e. TMD-2, MTMD-4 and STMD-4). Here, TMD-2 system is assumed to contain single TMD at the each midspan (refer to Table 2). Fig. 10 indicates that the STMD-4 has slightly better effectiveness than TMD-2 with the same mass ratio in suppressing the maximum displacement response of the bridge due to high-speed trains. The maximum displacement can be reduced up to 41.4, 45.9 and 49.4 for TMD-2, MTMD-4 and STMD-4, respectively.

The vertical displacement and acceleration time histories of the bridge for the first critical speed (302.7 km/h) are illustrated in Figs. 11, respectively. The maximum displacement and acceleration at the second midspan are 15.141 mm and 0.686g without TMDs, 7.239 mm and 0.332g with STMD-4, and 8.039 mm and 0.366g with MTMD-4, respectively. The vibrations are reduced by 52.2% and 46.9% for the maximum displacement response and 51.6% and 46.6% for the maximum acceleration

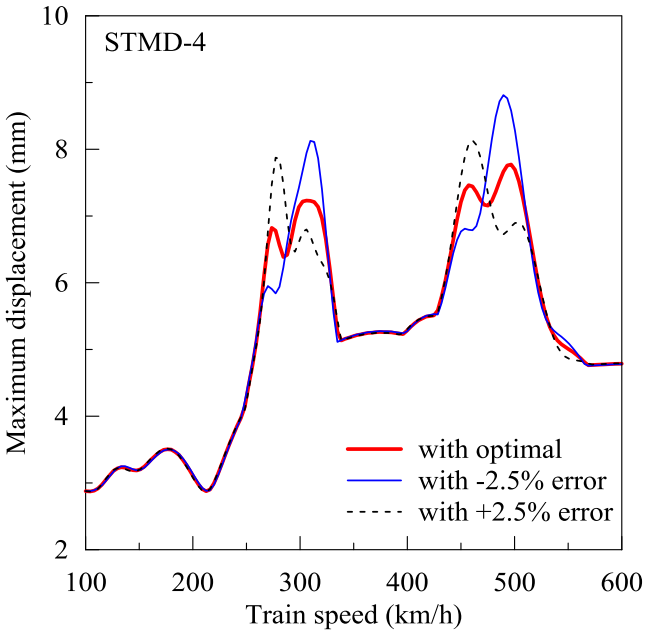

Fig. 12 Maximum displacements at the second midspan of the bridge with STMD-4 in case of detuning

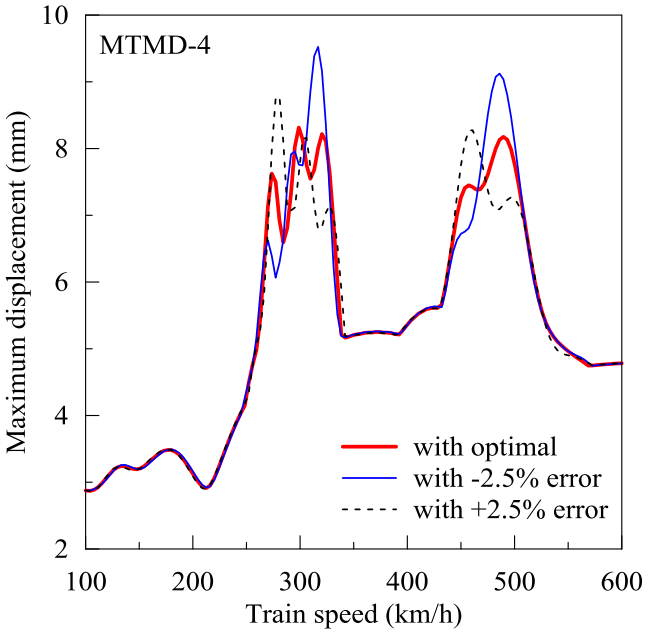

Fig. 13 Maximum displacements at the second midspan of the bridge with MTMD-4 in case of detuning

response with the installation of STMD-4 and MTMD-4, respectively. For railway bridge design, the maximum vertical acceleration must be smaller than 0.35g (Annex A2). Thus, MTMD-4 has a disadvantage for the considered bridge when compared to the STMD-4 system.

Maximum displacements at the second midspan with STMD-4 and MTMD-4 systems for 2.5% deviation from the optimum TMD frequency are shown in Figs. 12 and 13, respectively. As can be seen, a small deviation from the frequency tuning ratio causes detuning that results in large changes in the bridge response. According to these figures, the effectiveness of STMD-4 is better than that of MTMD-4.

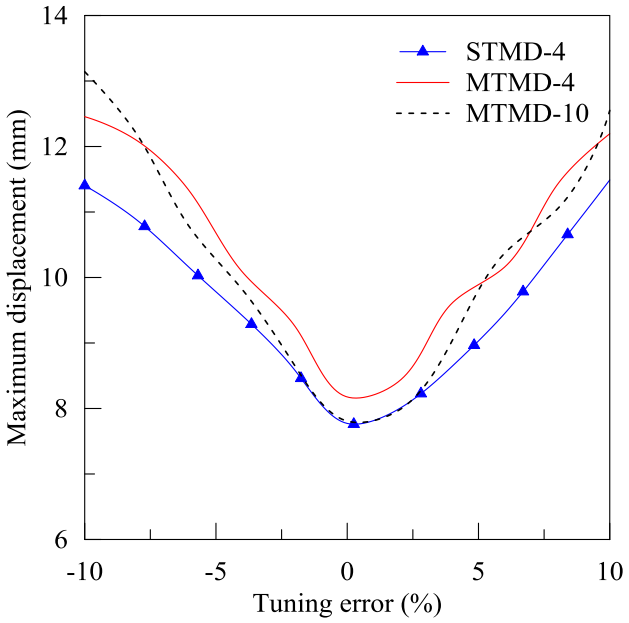

Fig. 14 Maximum displacements at the second midspan for different frequency tuning errors

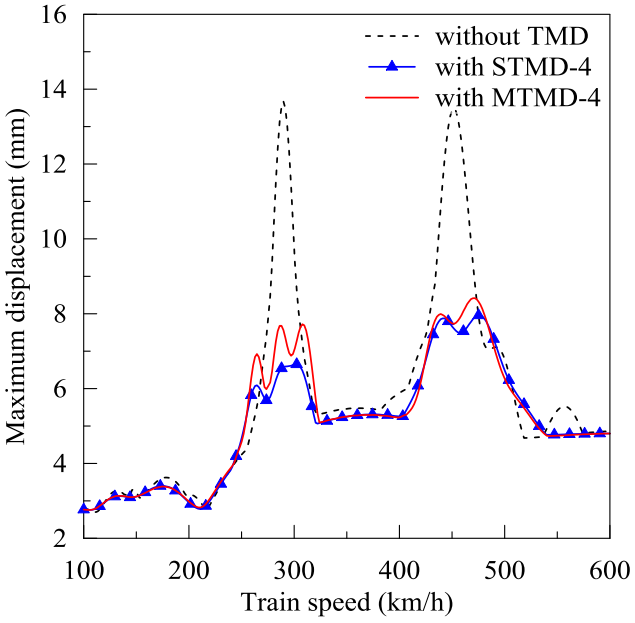

Fig. 15 Maximal displacements of the bridge with and without TMDs under HSLM-A7

The sensitivity of a system to a certain parameter is determined by comparing the optimal case with those obtained using variations of the parameters of interest. In this study, the robustness of the STMD system is examined for optimum tuning frequency, i.e. the rest of the parameters except the one examined are the optimum values for STMD system. As an example of such a detuning, a reduction of the TMD's optimum tuning frequency ratio by 5% is considered which has been simulated by reducing the TMD's stiffness to 90.25% of the optimal value. The formula of tuning error is expressed by Error % = (f_d - f_{opt}) / f_{opt}. Here, f_{opt} is optimum tuning frequency ratio and f_d is detuned frequency ratio.

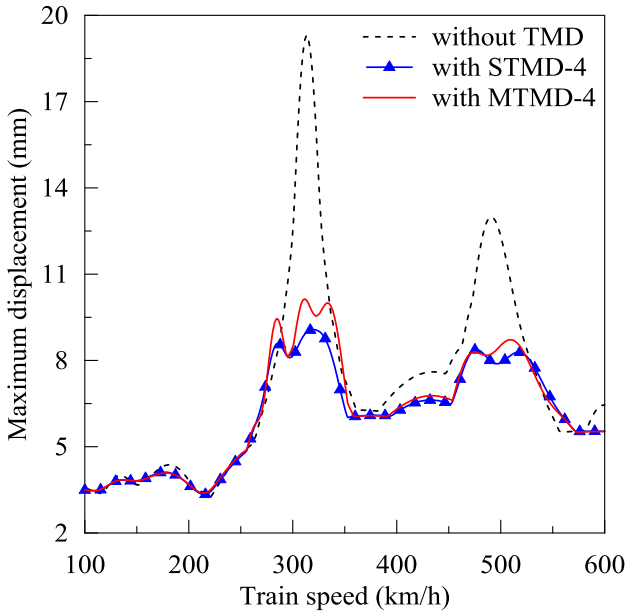

Fig. 16 Maximal displacements of the bridge with and without TMDs under HSLM-A9

To evaluate the robustness of three TMD devices, Fig. 14 shows comparison of three different tuned mass dampers (STMD-4, MTMD-4 and MTMD-10) when the frequency detuning ratios change between -10 and +10. The abscissa is the error from the estimated tuning frequency ratio of the TMD unit while the ordinate is the maximum displacement. As can seen, the dynamic response of the bridge system increases if the tuning frequency ratio is either increased or decreased in comparison with the optimal value. Fig. 14 also indicates that STMD-4 designed by using the SQP technique is the best in terms of the robustness compared to the others for the frequency detuning in greater than 2.5%.

In order to improve the generality of the STMD control effectiveness, the bridge with TMDs are also analyzed under different rail loading scenarios. HSLM-A7 and HSLM-A9 trains are used in numerical analysis, which defined in Eurocode 1. The maximum displacement curves of the bridge under trains with speeds ranging from 100 to 600 km/h are illustrated in Figs. 15 and 16. Compared with MTMD-4, the STMD is shown to be more effective in reducing the dynamic bridge responses when the train travels at critical speeds for both train models.

5. Conclusions

Series tunes mass dampers for suppression of multiple resonant peaks of continuous railway bridges under high-speed trains are presented in this study. A two-span bridge is considered as the case study. HSLM-A8 high-speed train model is used in numerical analyses, which is one of the high-speed passenger train models in Eurocode 1. The SQP technique is used for optimum parameters of STMD. Comparisons with several types of multiple tuned dampers available in the literature are made in terms of the control effectiveness and robustness. The following conclusions can be drawn from the study:

- In multi-span continuous bridges, it is observed the resonance peaks up to the number of spans, e.g., for a two-span bridge, there is two resonant peaks. Therefore, the number of MTMD or STMD devices to be installed on the bridge should not be smaller than the number of resonant peaks for effective vibration control.
- For continuous bridges, the first few modes of vibration not smaller than the number of spans is enough for the design of STMDs.
- Optimum location of STMDs is on the middle of each span.
- For the first TMD unit in a STMD, optimal damping is always obtained to be zero.
- For optimal case, i.e., no detuning, both STMDs and MTMDs show the approximately same control effectiveness.
- The optimal STMD-4 achieves approximately the same level of response reduction as the optimum MTMD-10. Thus, STMDs are more economic and advanced control devices than MTMDs.
- STMD's effectiveness is better than that of the MTMDs considered when the shift (or detuning) of the frequency tuning ratio is larger than 2.5%.

References

Adam, C. and Salcher, P. (2014), "Dynamic effect of high-speed trains on simple bridge structures", *Struct. Eng. Mech.,* **51**(4), 581-599. https://doi.org/10.12989/sem.2014.51.4.581.

Asami, T. (2017), "Optimal design of double-mass dynamic vibration absorbers arranged in series or in parallel", *J. Vib. Acoust*., **139**(1), 011015. https://doi.org/10.1115/1.4034776.

Asami, T., Mizukawa, Y. and Ise, T. (2018), "Optimal design of double-mass dynamic vibration absorbers minimizing the mobility transfer function", *J. Vib. Acoust*., **140**(6), 061012. https://doi.org/10.1115/1.4040229.

CSI Computers & Structures Inc, SAP2000, Integrated Software for Structural Analysis & Design, Version 15.1, CSI Inc, Berkeley, California, USA, 2010.

European Committee for Standardization, Basis of Structural Design Annex A2: Application for Bridges, Final PT Draft EN 1990-prAnnex A2, 2002.

European Committee for Standardization, Eurocode 1: Actions on Structures - Part 2: Traffic Loads on Bridge, 2003.

Giaralis, A. and Petrini, F. (2017), "Wind-Induced Vibration Mitigation in Tall Buildings Using the Tuned Mass-Damper-Inerter", *J. Struct. Eng.*, **143**, 04017127. https://doi.org/10.1061/(ASCE)ST.1943-541X.0001863.

Kahya, V. and Araz, O. (2017), "Series tuned mass dampers in train-induced vibration control of railway bridges", *Struct. Eng. Mech.,* **61**(4), 453-461.
https://doi.org/10.12989/sem.2017.61.4.453.

Li, C. and Zhu, B. (2006), "Estimating double tuned mass dampers for structures under ground acceleration using a novel optimum criterion", *J. Sound Vib*., **298**, 280-297. https://doi.org/10.1016/j.jsv.2006.05.018.

Li, J., Su, M. and Fan, L. (2005), "Vibration control of railway bridges under high-speed trains using multiple tuned mass dampers", *J. Bridge Eng*., **10**, 312-320. https://doi.org/10.1061/(ASCE)1084-0702(2005)10:3(312).

Luu, M., Martinez-Rodrigo, M. D., Zabel, V. and Könke, C. (2014), "H∞ optimization of fluid viscous dampers for reducing vibrations of high-speed railway bridges", *J. Sound Vib*., **333**(9), 2421-2442. https://doi.org/10.1016/j.jsv.2013.12.030.

Luu, M., Zabel, V. and Könke, C. (2012), "An optimization method of multi-resonant response of high-speed train bridges using TMDs", *Finite Elem. Anal. Des*., **53**, 13-23. https://doi.org/10.1016/j.finel.2011.12.003.

MATLAB optimization toolbox user's guide R2015b, MathWorks, Natick, MA, 2015.

Miguel, L. F. F., Lopez, R. H., Torii, A. J., Miguel, L. F. F. and Beck, A. T. (2016), "Robust design optimization of TMDs in vehicle–bridge coupled vibration problems", *Eng. Struct*., **126**, 703-711. https://doi.org/10.1016/j.engstruct.2016.08.033.

Moghaddas, M., Esmailzadeh, E., Sedaghati, R. and Khosravi, P. (2012), "Vibration control of Timoshenko beam traversed by moving vehicle using optimized tuned mass damper", *J. Vib. Control*., **18**(6), 757-773.
https://doi.org/10.1177/1077546311404267.

Podworna, M. (2017), "Dynamic response of steel-concrete composite bridges loaded by high-speed train", *Struct. Eng. Mech.,* **62**(2), 179-196. https://doi.org/10.12989/sem.2017.62.2.179.

Rostam, M. R., Javid, F., Esmailzadeh, E. and Younesian, D. (2015), "Vibration suppression of curved beams traversed by off-center moving loads", *J. Sound Vib.*, **352**, 1-15. https://doi.org/10.1016/j.jsv.2015.04.038.

Ruiz, R., Taflanidis, A.A., Giaralis, A. and Lopez-Garcia, D. (2018), "Risk-informed optimization of the tuned mass-damper-inerter (TMDI) for the seismic protection of multi-storey building structures", *Eng. Struct.*, **177**, 836-850. https://doi.org/10.1016/j.engstruct.2018.08.074.

Samani, F. S., Pellicano, F. and Masoumi, A. (2013), "Performances of dynamic vibration absorbers for beams subjected to moving loads", *Nonlinear Dyn*., **73**, 1065-1079. https://doi.org/10.1007/s11071-013-0853-4.

Wang, J. F., Lin, C. C. and Chen, B. L. (2003), "Vibration suppression for high-speed railway bridges using tuned mass dampers", *Int. J. Solids Struct*., **40**(2), 465-491. https://doi.org/10.1016/S0020-7683(02)00589-9.

Wang, Y., Wei, Q. C., Shi, J. and Long, X. (2010), "Resonance characteristics of two-span continuous beam under moving high-speed trains", *Lat. Am. J. Solid Struct.*, **7**, 185-199. http://dx.doi.org/10.1590/S1679-78252010000200005.

Wu, J. J. (2006), "Study on the inertia effect of helical spring of the absorber on suppressing the dynamic responses of a beam subjected to a moving load", *J. Sound Vib*., **297**, 981-999. https://doi.org/10.1016/j.jsv.2006.05.011.

Xu, K., Bi, K., Han, Q., Li, X. and Du, X. (2019), "Using tuned mass damper inerter to mitigate vortex-induced vibration of long-span bridges: Analytical study", *Eng. Struct.*, **182**, 101-111. https://doi.org/10.1016/j.engstruct.2018.12.067.

Yau, J. D., Wu, Y. S. and Yang, Y. B. (2001), "Impact response of bridges with elastic bearings to moving loads", *J. Sound Vib*., **248**(1), 9-30. https://doi.org/10.1006/jsvi.2001.3688.

Yau J. D. and Yang, Y. B. (2004a), "Vibration reduction for cable-stayed bridges traveled by high-speed trains", *Finite Elem. Anal. Des*., **40**, 341-359. https://doi.org/10.1016/S0168-874X(03)00051-9.

Yau J. D. and Yang, Y. B. (2004b), "A wideband MTMD system for reducing the dynamic response of continuous truss bridges to moving train loads", *Eng. Struct*., **26**, 1795-1807. https://doi.org/10.1016/j.engstruct.2004.06.015.

Zuo, L. (2009), "Effective and robust vibration control using series multiple tuned-mass dampers", *J. Vib. Acoust.*, **131**(3), 031003. https://doi.org/10.1115/1.3085879.

CC